

## Supporting Information

### Enzymatic Activation of Nitro-Fluorogens in Live Bacterial Cells for Enzymatic Turnover Activated Localization Microscopy

Marissa K. Lee,<sup>†</sup> Jarrod Williams,<sup>‡</sup> Robert J. Twieg,<sup>‡</sup> Jianghong Rao,<sup>§</sup> and W.E. Moerner<sup>\*,†</sup>

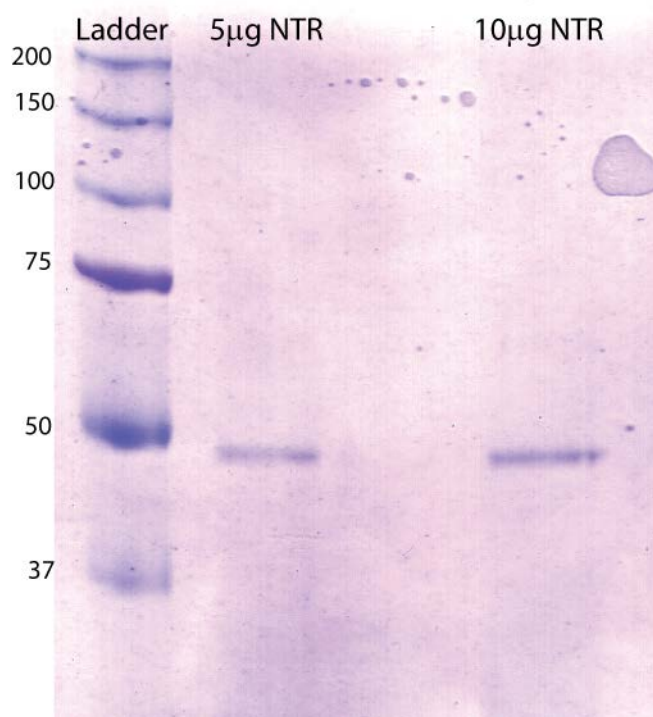
<sup>†</sup>*Department of Chemistry, Stanford University, Stanford, California, 94305*

<sup>‡</sup>*Department of Chemistry, Kent State University, Kent, Ohio 44244*

<sup>§</sup>*Department of Radiology, Stanford University, Stanford, California, 94305*

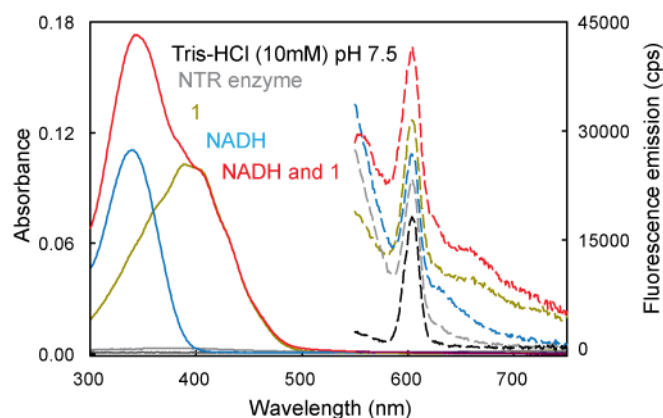
#### Table of Contents

Figure S1. Protein gel purity of NTR enzyme. ....	2
Figure S2. NTR enzyme, NADH and 1 are all required for fluorescence turn-on. ....	2
Figure S3. Photograph of NTR reaction. ....	3
Figure S4. Compound 4 reduced into fluorescent products by NTR enzyme. ....	3
Figure S5. Compound 5 is reduced into fluorescent product by NTR enzyme. ....	4
Figure S6. Controls for <i>in vitro</i> NTR reaction of 4 on poly-lysine coated coverslips. ....	4
Figure S7. SM time traces of compound 2 in polymer ....	5
Figure S8. Compounds 1 and 5 have similar kinetics in low concentration regime. ....	5
Figure S9. Fluorescence turn-on with other species of bacteria. ....	6
Table S1. Photophysical characterization of compounds 4 and 5. ....	6
Movie S1. Single molecules of compound 2 in PVA polymer film. ....	6
Movie S2. Single molecules generated in <i>B. subtilis</i> . ....	6
Materials and Methods. ....	7
Synthesis schemes. ....	7
Synthesis and characterization. ....	9
Bulk spectroscopy. ....	16
<i>In vitro</i> sample preparation and analysis. ....	17
Microscopy. ....	18
Live-cell imaging and analysis. ....	18
References. ....	20
Proton NMR spectra. ....	21



**Figure S1.** Protein gel purity of NTR enzyme.

Gel electrophoresis on NTR enzyme (>90% purity, Sigma Aldrich) showing expected molecular weight of 48 kDa (corresponding to dimers of the 24 kDa monomers) and purity. Protein gel is 12% SDS-PAGE with Precision Plus ladder and stained with Coomassie Brilliant Blue and was obtained with the help of Steffi Duttler in the Frydman lab.



**Figure S2.** NTR enzyme, NADH and **1** are all required for fluorescence turn-on.

Solid lines represent the absorbance of NTR enzyme, **1**, NADH, and NADH with **1** in Tris-HCl (10 mM pH 7.5), (gray, yellow, blue, and red, respectively). The corresponding fluorescence emission (pumped at 500 nm) is shown as dashed lines with same color scheme. The sharp peak at 604 nm was shown to be Raman scattering by shifting the pumping wavelength +/- 5 nm. The

absorbance and fluorescence emission of NTR enzyme with **1** or with NADH overlap closely with the spectra for **1** or NADH (respectively) and are not shown for space considerations.

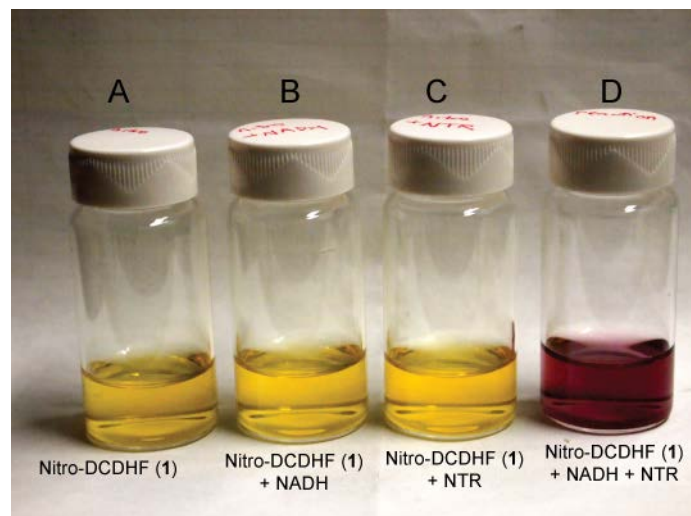


**Figure S3.** Photograph of NTR reaction.

Photograph of equimolar samples of (A) nitro fluorogen **1** (~mM) in Tris-HCl (10 mM pH 7.5), (B) **1** and excess NADH, (C) **1** and NTR (~10 nM) and (D) **1**, excess NADH and NTR showing color shift after NTR reaction has completed. All vials allowed to incubate for 10 minutes before photograph was taken.

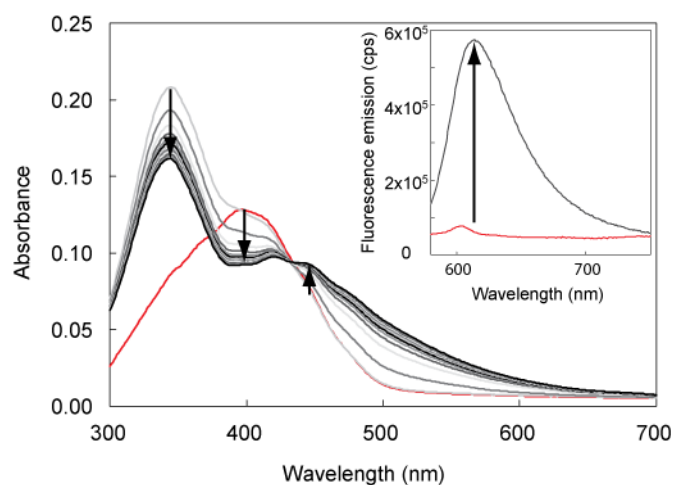


**Figure S4.** Compound **4** reduced into fluorescent products by NTR enzyme.

Spectral change during the NTR reaction with **4** and NADH over  $\approx 10$  minutes showing red-shifted emission and fluorescence increase. Gray curves show absorbance at different time points, red curve is the absorbance of **4** alone. Inset: Fluorescence emission (500 nm excitation) before and after NTR reaction. No fluorescence turn-on observed without all three components. Spectra measured in PBS (pH 7.4).

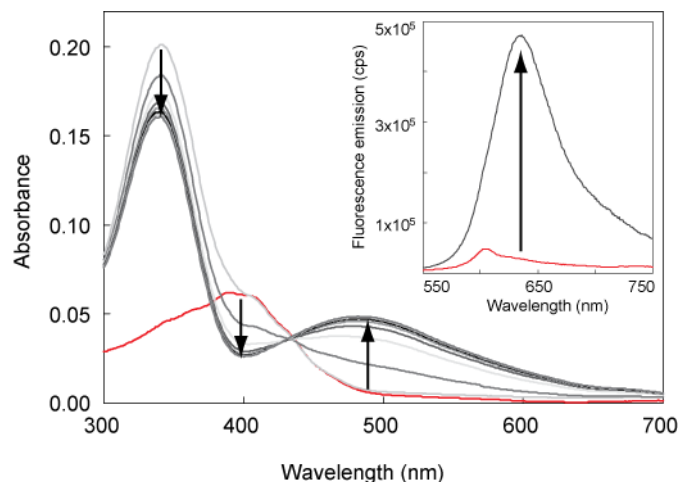


**Figure S5.** Compound **5** is reduced into fluorescent product by NTR enzyme. Spectral change during the NTR reaction with **5** and NADH over  $\approx 10$  minutes showing red-shifted emission and fluorescence increase. Gray curves show absorbance at different time points, red curve is the absorbance of **5** alone. Inset: Fluorescence emission (500 nm excitation) before and after NTR reaction. No fluorescence turn-on observed without all three components. Spectra measured in PBS (pH 7.4).

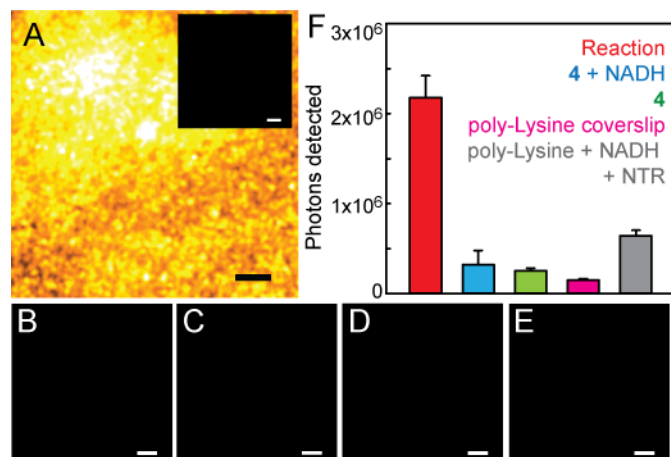


**Figure S6.** Controls for *in vitro* NTR reaction of **4** on poly-lysine coated coverslips. (A) Bulk fluorescence of **4** attached to poly-lysine surface and immersed in PBS (pH 7.4) after NADH and NTR addition. Inset: Bulk fluorescence of **4** before NADH and NTR addition at some contrast as (A). Images (B) through (E) bulk fluorescence images at same contrast as (A). (B) Compound **4** attached to poly-lysine slides with NADH. (C) Compound **4** attached to poly-lysine slides with NTR enzyme. (D) Poly-lysine coated coverslip without **4**. (E) Poly-lysine coated coverslip with NADH and NTR added. (F) Average photons detected per pixel for each incubation condition. All scale bars are 2  $\mu\text{m}$ . See Materials and Methods section for more details about sample preparation.

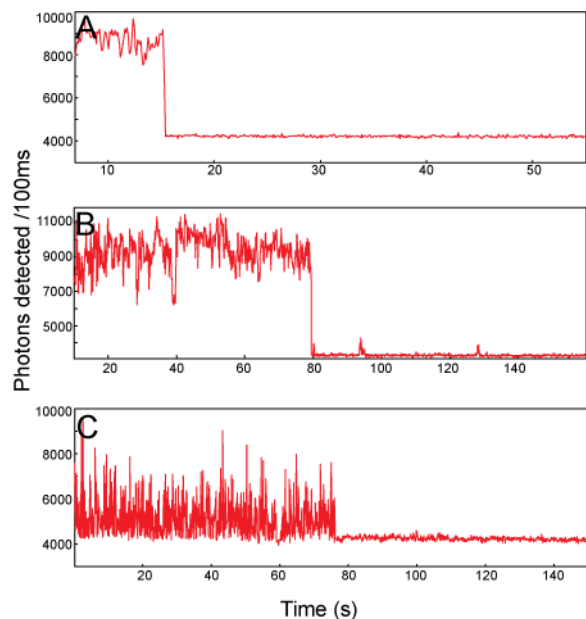


**Figure S7.** SM time traces of compound **2** in polymer  
The SM traces of compound **2** doped into PVA polymer film at nM concentration show blinking at a variety of intensities. The blinking becomes more pronounced at higher intensities. The intensities are (A)  $376 \text{ W/cm}^2$ , (B)  $783 \text{ W/cm}^2$ , (C)  $1590 \text{ W/cm}^2$ .

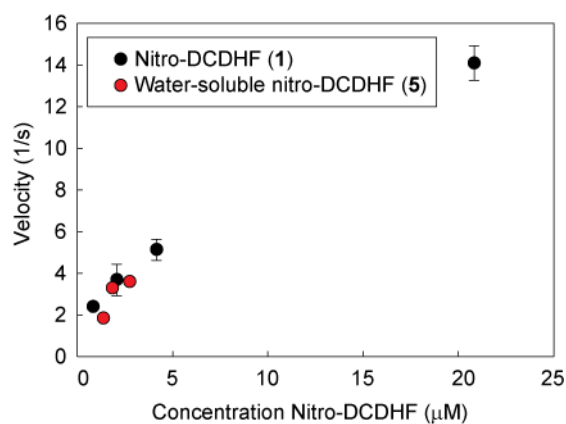


**Figure S8.** Compounds **1** and **5** have similar kinetics in low concentration regime.  
The initial rate of formation of **2** was measured by the change in absorbance at 500 nm for **1** and **5** in the low concentration regime ( $<10 \mu\text{M}$ ) at the same NADH concentration ( $\sim 10 \mu\text{M}$ ) in PBS (pH 7.4). In this regime, **1** and **5** behave similarly, but at higher concentrations, **1** aggregates. The full data for the entire concentration regime for **5** is shown in figure 3.

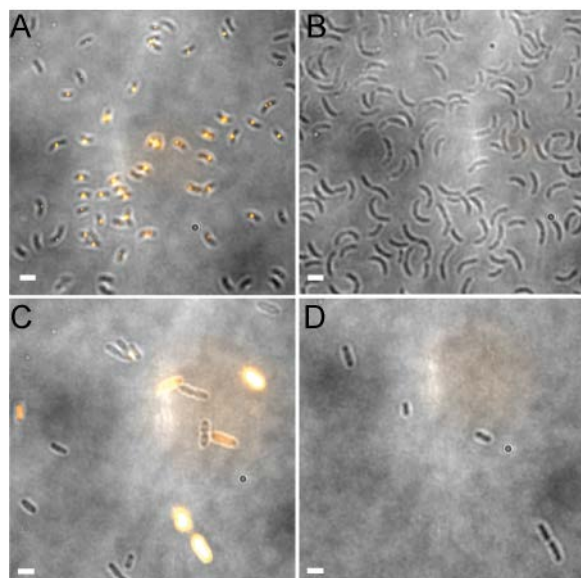


**Figure S9.** Fluorescence turn-on with other species of bacteria. (A) through (D) are composite images overlaying the average fluorescence with the white light image of cells. (A) *C. crescentus* incubated with 2.5  $\mu\text{M}$  **1** and 5% DMSO for 30 minutes. (B) *C. crescentus* incubated with 5% DMSO for 30 minutes. (C) *E. coli* incubated with 2.5  $\mu\text{M}$  **1** and 5% DMSO for 30 minutes. (D) *E. coli* incubated with 5% DMSO for 30 minutes. All cells were washed 5x before imaging (532 nm excitation, 576 W/cm<sup>2</sup>) Scale bars are 2  $\mu\text{m}$ .

**Table S1.** Photophysical characterization of compounds **4** and **5**.

	$\lambda_{\text{abs}}$ (nm)	$\epsilon$ (M <sup>-1</sup> cm <sup>-1</sup> )	$\lambda_{\text{fl}}$ (nm)
<b>4</b> <sup>a</sup>	395	22500	n/a
<b>5</b> <sup>b</sup>	390	22600	n/a

<sup>a</sup>Measured in PBS, pH 7.4

<sup>b</sup>Measured in 10mM Tris-HCl, pH 7.5

**Movie S1.** Single molecules of compound **2** in PVA polymer film.

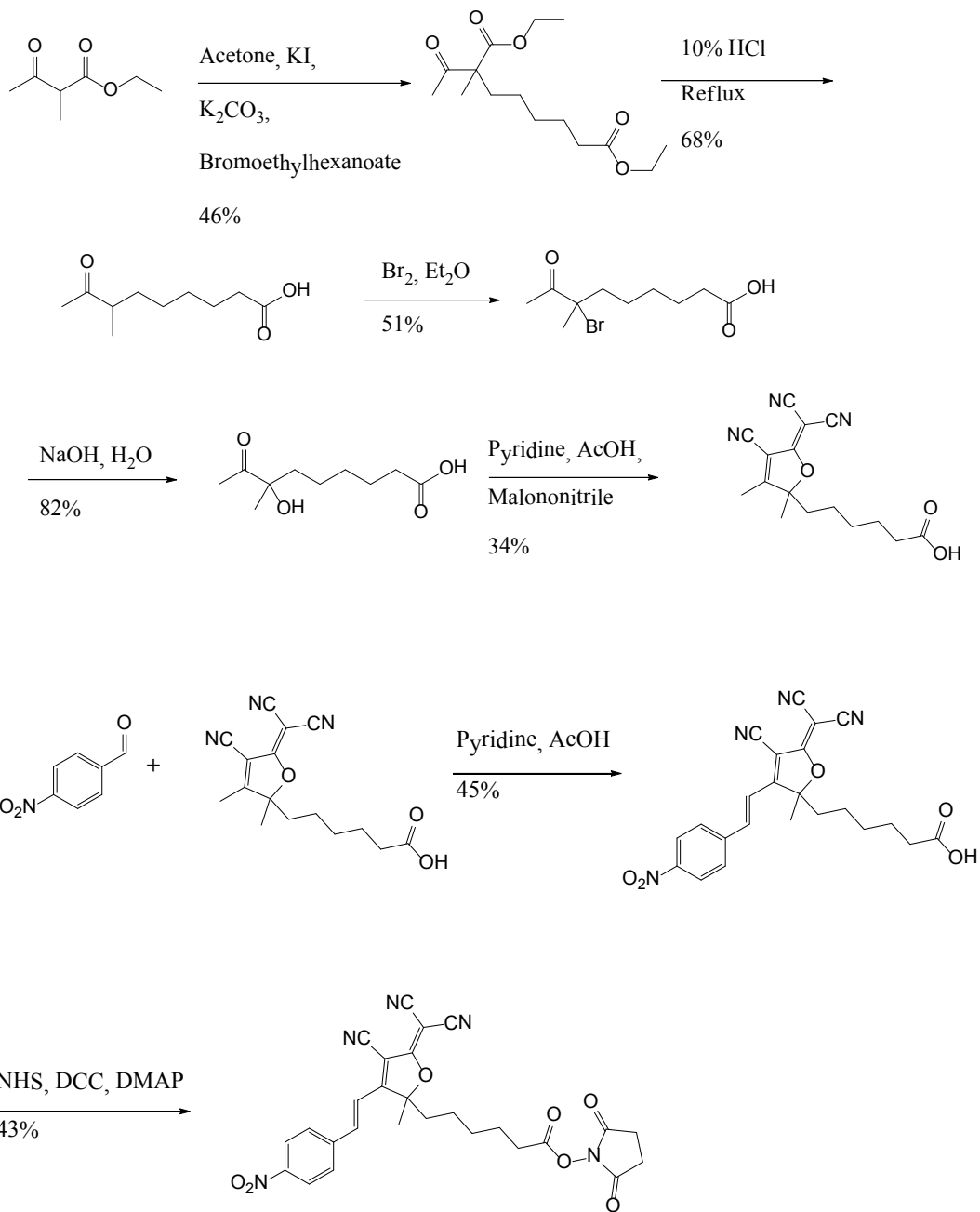
Imaging **2** embedded in PVA polymer with 532 nm (91 W/cm<sup>2</sup>) with 100 ms integration time (10 frames per second). Scale bar is 2  $\mu\text{m}$ .

**Movie S2.** Single molecules generated in *B. subtilis*.

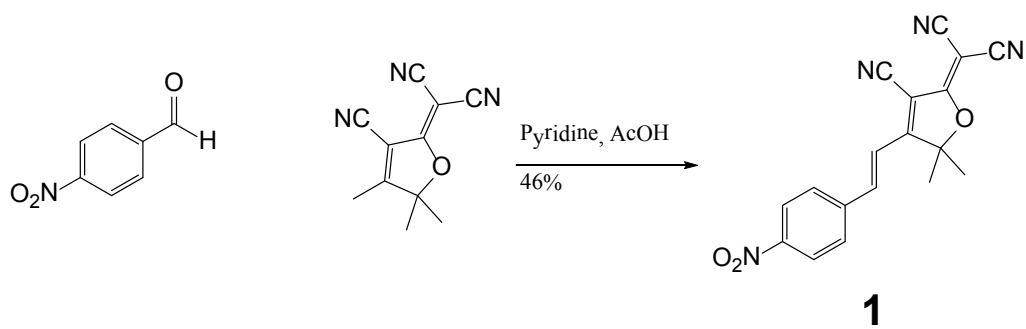
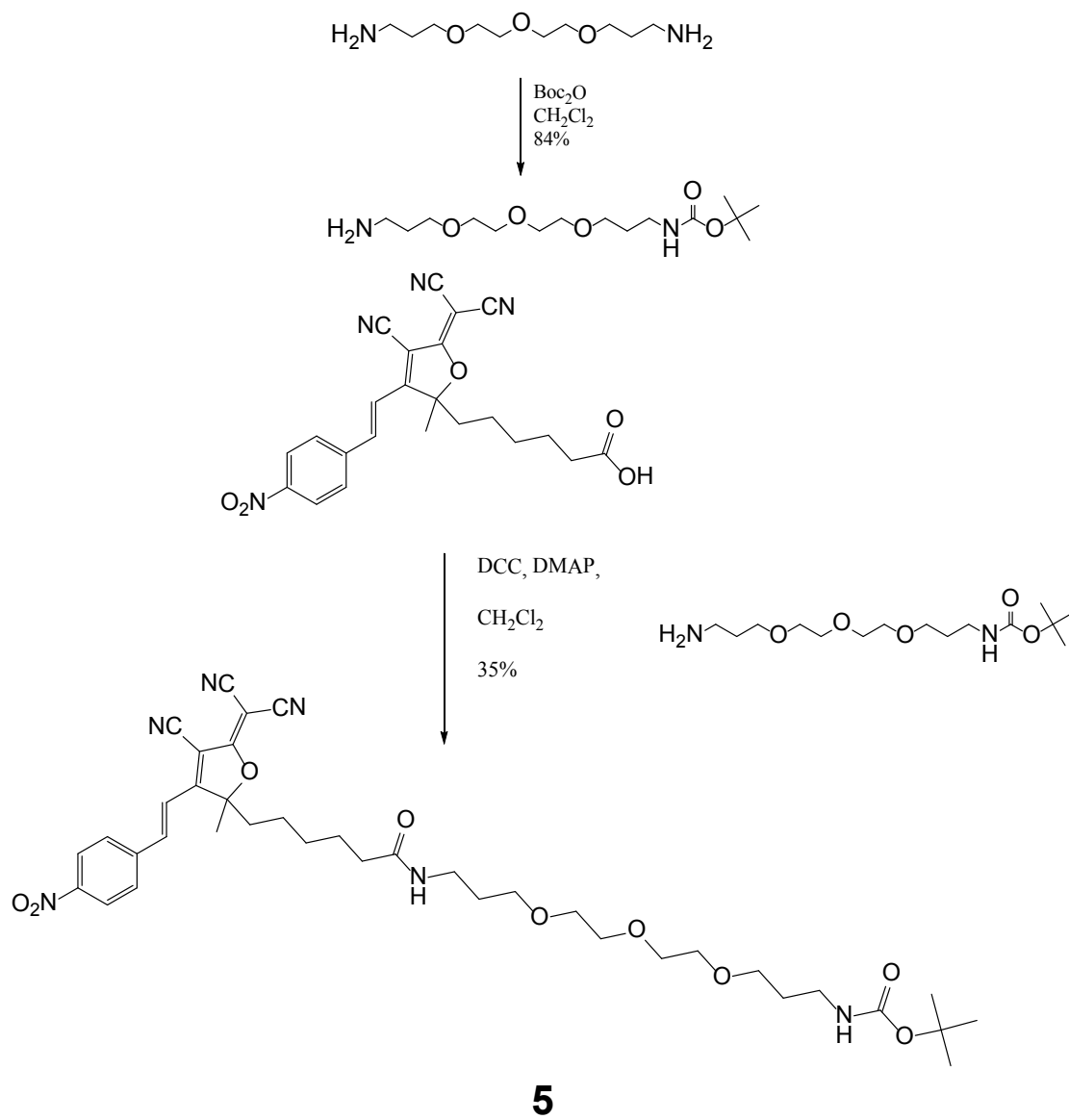
Movie of SMs in *B. subtilis* from Figure 5B (incubated with 1 nM **1**) and imaged with 532 nm (15 kW/cm<sup>2</sup>, 8 ms integration time, 125 frames per second). Movie is slowed down ~10x to be 13 frames per second. Scale bar is 2  $\mu\text{m}$ .

## Materials and Methods

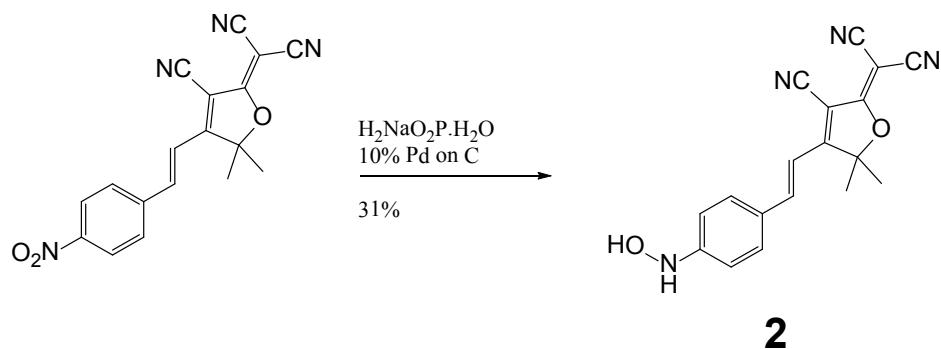
### Synthesis schemes



**4**



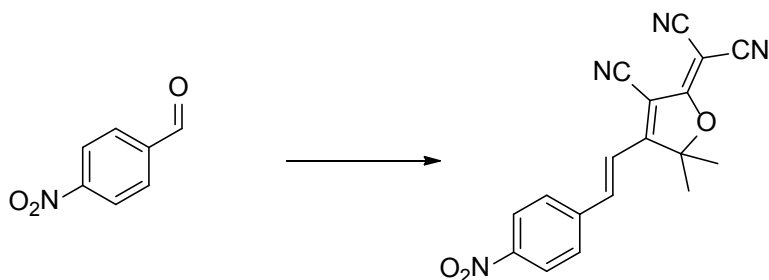




### Synthesis and characterization

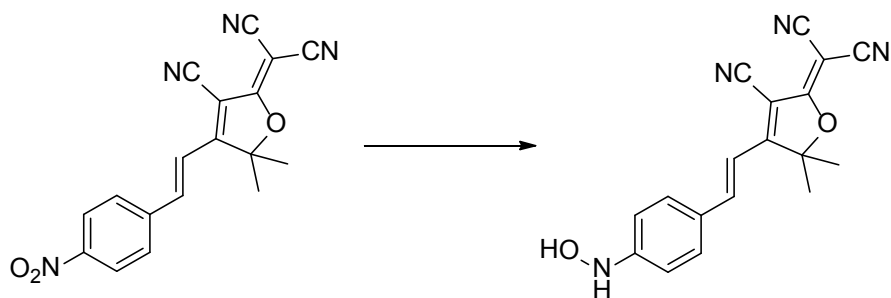
The synthesis and characterization of compounds **1** and **3** have already been reported.<sup>1</sup> Here an alternative synthetic procedure was followed for **1**.

2-{3-Cyano-5,5-dimethyl-4-[2-(4-nitro-phenyl)-vinyl]-5H-furan-2-ylidene}-malononitrile (**1**).



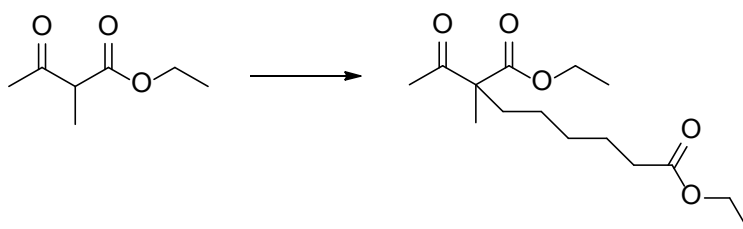
To a 100-mL round bottom flask with stirbar was added 4-nitrobenzaldehyde (0.30 g, 2.00 mmol), 2-(3-cyano-4,5,5-trimethyl-5H-furan-2-ylidene)-malononitrile<sup>2</sup> (0.40 g, 2.00 mmol), pyridine (5 mL) and acetic acid (several drops). After stirring at room temperature for 2.5 days, TLC showed the desired nitro product had been formed in substantial quantity. The reaction was poured into ice-water (1 L), stirred for 2 h and the precipitate was removed by suction filtration. The solid was recrystallized from 1-propanol to give 2-{3-cyano-5,5-dimethyl-4-[2-(4-nitro-phenyl)-vinyl]-5H-furan-2-ylidene}-malononitrile<sup>1</sup> as a dark solid (0.30 g, 46% yield). This compound begins decomposing near 270 °C prior to melting at 280 °C. When cooled and reheated to 280 °C, the material becomes darker and shows more signs of decomposition as the melting point is reached. Mp 281 °C. IR (neat, cm<sup>-1</sup>): 3084, 2220, 1581, 1521, 1345, 1105; <sup>1</sup>H NMR (400 MHz, DMSO) δ 8.32 (d, 2.0 Hz, 8.8 Hz), 8.17 (d, 2H, 8.8 Hz), 7.96 (d, 1H, 16.4 Hz), 7.39 (d, 1H, 16.4 Hz), 1.82 (s, 6H); <sup>13</sup>C NMR (400 MHz, CDCl<sub>3</sub>) δ 171.9, 149.6, 143.2, 139.4, 129.3, 124.6, 118.5, 110.9, 110.1, 109.6, 97.7, 26.2.

2-{3-Cyano-4-[2-(4-hydroxyamino-phenyl)-vinyl]-5,5-dimethyl-5H-furan-2-ylidene}-malononitrile (**2**).



To a 2 neck round bottom flask equipped with a condenser, stirbar and nitrogen inlet was added 2-(3-cyano-5,5-dimethyl-4-[2-(4-nitro-phenyl)-vinyl]-5H-furan-2-ylidene)-malononitrile (0.10 g, 0.30 mmol), and 6 mL of THF. A solution of sodium hypophosphite monohydrate (0.08 g, 0.76 mmol) in 6 mL of water was added and the mixture was cooled to 5°C. Palladium on carbon (10%, 0.06 g) was added and the cooling bath was removed. The solution was then heated with stirring at 40°C for 1 hour while being monitored by thin layer chromatography (75% EtOAc, 25% hexane). Once the starting material had disappeared the reaction was filtered, added to 50 mL of ethyl acetate and rinsed with an equal volume of water. Purification by column chromatography (75% EtOAc, 25% hexane) gave 0.03 g of 2-(3-cyano-4-[2-(4-hydroxyamino-phenyl)-vinyl]-5,5-dimethyl-5H-furan-2-ylidene)-malononitrile as a dark purple solid. (Yield: 31%). IR (neat,  $\text{cm}^{-1}$ ): 3298, 2988, 2935, 2225, 2166, 1552, 1518, 1459, 1396, 1379, 1344, 1314, 1280, 1229, 1168, 1105, 1011, 966, 915, 868;  $^1\text{H}$  NMR (400 MHz, DMSO)  $\delta$  9.68 (s, 1H), 9.08 (s, 1H), 7.90 (d, 1H, 16.0 Hz), 7.77 (d, 2H, 8.8 Hz), 6.92 (d, 1H, 16.0 Hz), 6.84 (d, 2H, 8.8 Hz), 1.76 (s, 6H);  $^{13}\text{C}$  NMR (400 MHz, DMSO)  $\delta$  177.82, 176.12, 156.22, 149.70, 132.99, 124.56, 113.80, 112.97, 112.27, 111.78, 109.71, 98.92, 70.25, 26.08; HRMS  $m/z$  Calcd. For  $\text{C}_{18}\text{H}_{14}\text{N}_4\text{O}_2$  (M+Na): 341.1014. Found: 341.1021; Mp: decomposes over 300 °C.

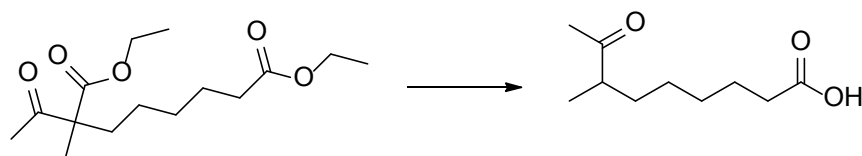
#### 2-Acetyl-2-methyl-octanedioic acid diethyl ester



To a stirred solution of 2-methylethylacetoacetate (22.97 g, 0.159 mol) in acetone (200 mL) was added potassium carbonate (47.05 g, 0.341 mol) and potassium iodide (7.40 g, 0.446 mol) at room temperature. After stirring for 10 minutes, a solution of 6-bromoethylhexanoate (32.00 g, 0.143 mol) in 100 mL of acetone was added and the mixture was allowed to reflux for 24 hours before being cooled to room temperature. The solids were removed by vacuum filtration and the solvent was removed under reduced pressure. The resulting oil was dissolved in ethyl acetate and washed once with water. The organic phase was separated, dried over magnesium sulfate and rotovapped to a yellow oil. The more volatile starting materials were removed by kugelrohr

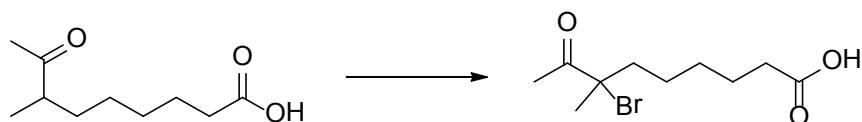
distillation (0.05 mm Hg, 75°C) while the composition of the mixture was being monitored by GC/MS. The final weight of the pure 2-acetyl-2-methyl-octanedioic acid diethyl ester<sup>3</sup> was 21.04 g. (Yield: 46%). IR (neat, cm<sup>-1</sup>): 2980, 2931, 2860, 1732, 1712, 1463, 1374, 1355, 1299, 1241, 1175, 1153, 1005, 1066, 1025, 858; <sup>1</sup>H NMR (400 MHz, CDCl<sub>3</sub>) δ 4.21 (q, 2H, 7.2 Hz), 4.14 (q, 2H, 7.2 Hz), 2.29 (t, 2H, 7.2 Hz), 2.15 (s, 3H), 1.90 (m, 1H), 1.75 (m, 1H), 1.64 (m, 2H), 1.35 (m, 5H), 1.26 (m, 6H), 1.20 (m, 2H); <sup>13</sup>C NMR (400 MHz, CDCl<sub>3</sub>) δ 205.8, 173.7, 173.0, 61.2, 60.2, 59.6, 34.6, 34.2, 29.4, 26.1, 24.6, 23.9, 18.8, 14.2, 14.0; HRMS *m/z* Calcd. for C<sub>15</sub>H<sub>26</sub>O<sub>5</sub> (M+Na): 309.1678. Found: 309.1690.

### 7-Methyl-8-oxo-nonanoic acid



To 300 ml of 10% aqueous HCl was added 2-acetyl-2-methyl-octanedioic acid diethyl ester (21.04 g, 73.52 mmol). The resulting mixture was allowed to reflux for 24 hours. After cooling to room temperature, it was carefully neutralized and then made basic with saturated sodium bicarbonate solution. It was then extracted once with diethyl ether to remove any of the ester byproducts and unreacted starting material. The aqueous phase was separated, made acidic again with 4M HCl and extracted with diethyl ether (~300 mL). The organic phase was dried over magnesium sulfate and rotovapped to dryness leaving pure 7-methyl-8-oxo-nonanoic acid<sup>3</sup> as a yellow oil (9.36 g, 68%). IR (neat): 3495, 2934, 2860, 1703, 1459, 1414, 1357, 1268, 1227, 1175, 1152, 1115, 948, 841; <sup>1</sup>H NMR (400 MHz, CDCl<sub>3</sub>) δ 2.52 (m, 1H), 2.36 (t, 2H, 7.2 Hz), 2.15 (s, 3H), 1.67 (m, 3H), 1.40-1.25 (m, 5H), 1.09 (d, 3H, 6.8 Hz); <sup>13</sup>C NMR (400 MHz, CDCl<sub>3</sub>) δ 212.9, 179.6, 47.1, 33.9, 32.6, 29.0, 28.0, 26.9, 24.5, 16.3; HRMS *m/z* Calcd. for C<sub>10</sub>H<sub>18</sub>O<sub>3</sub> (M+Na): 209.1154. Found: 209.1149.

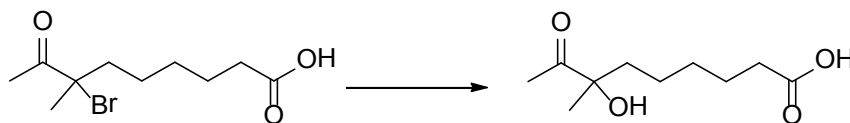
### 7-Bromo-7-methyl-8-oxo-nonanoic acid



To a stirred solution of 7-methyl-8-oxo-nonanoic acid (8.50 g, 45.63 mmol) in diethyl ether (200 mL) was added bromine (7.29 g, 45.61 mmol) dropwise over the course of 60 minutes. The resulting dark red solution rapidly turned to a light orange and was allowed to stir overnight at room temperature. The reaction mixture was then washed 3 times with 200 mL of water. The organic phase was dried over magnesium sulfate and the diethyl ether was removed under

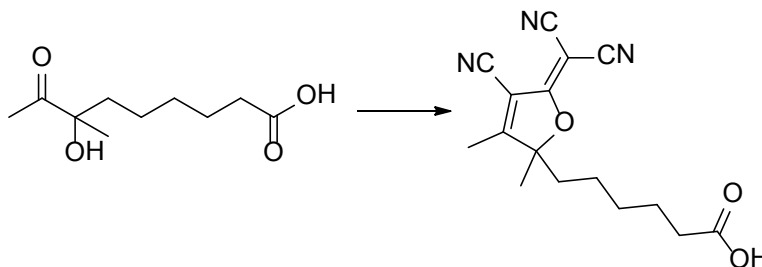
reduced pressure to give 11.00 g of a light green oil. Purification by column chromatography (60% CH<sub>2</sub>Cl<sub>2</sub>, 38% hexane, 2% acetic acid) gave 5.11 g of 7-bromo-7-methyl-8-oxo-nonanoic acid as a clear oil. (Yield 51%). IR (neat, cm<sup>-1</sup>): 3200, 2935, 2863, 1705, 1413, 1378, 1356, 1284, 1228, 1146, 1110, 1055, 934, 846, 730; <sup>1</sup>H NMR (400 MHz, CDCl<sub>3</sub>) δ 2.44 (s, 3H), 2.39 (t, 2H, 7.2 Hz), 2.13 (m, 1H), 2.01 (m, 1H), 1.83 (s, 3H), 1.68 (m, 2H), 1.55-1.25 (m, 4H); <sup>13</sup>C NMR (400 MHz, CDCl<sub>3</sub>) δ 203.7, 179.5, 69.3, 41.2, 33.7, 28.9, 26.6, 25.5, 24.9, 24.4; HRMS *m/z* Calcd. for C<sub>10</sub>H<sub>27</sub>BrO<sub>3</sub> (M+Na): 287.0259. Found: 287.0249.

#### 7-hydroxy-7-methyl-8-oxo-nonanoic acid



To a solution of sodium hydroxide (2.69 g, 67.34mmol) in 100 mL of water was added 7-bromo-7-methyl-8-oxo-nonanoic acid (5.76 g, 21.72 mmol). After stirring overnight at 60° C the mixture was cooled to room temperature and made acidic with 2M HCl. The solution was then extracted twice with diethyl ether (150 mL). The combined organic fractions were dried over magnesium sulfate and rotovaped to dryness. Purification by column chromatography (75% EtOAc, 25% hexane) gave 3.62 g of 7-hydroxy-7-methyl-8-oxo-nonanoic acid as a clear oil. (Yield: 82%). IR (neat, cm<sup>-1</sup>): 3432, 3162, 2936, 2862, 1704, 1457, 1412, 1355, 1277, 1234, 1166, 1114, 1059, 997, 963, 938, 888, 839, 776; <sup>1</sup>H NMR (400 MHz, CDCl<sub>3</sub>) δ 2.30 (t, 2H, 7.6 Hz), 2.19 (s, 3H), 1.66 (t, 2H, 8 Hz), 1.57 (m, 2H, 1.41 (m, 1H), 1.36, (s, 3H), 1.33 (m, 2H), 1.02 (m, 1H); <sup>13</sup>C NMR (400 MHz, CDCl<sub>3</sub>) δ 212.3, 179.4, 78.8, 39.1, 33.9, 29.1, 25.3, 24.4, 23.6, 22.9; HRMS *m/z* Calcd. for C<sub>10</sub>H<sub>18</sub>O<sub>4</sub> (M+Na): 225.1103. Found: 225.1119.

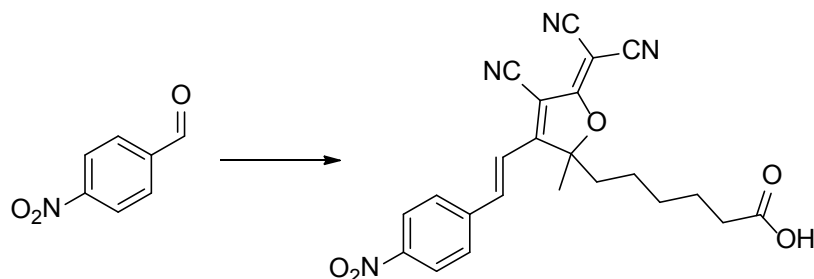
#### 6-(3-Cyano-4-dicyanomethylene-1,2-dimethyl-cyclopent-2-enyl)-hexanoic acid



To a solution of 7-hydroxy-7-methyl-8-oxo-nonanoic acid (3.58 g, 19.03 mmol) and malononitrile (3.03 g, 45.97 mmol) in anhydrous ethanol (50mL) was added sodium ethoxide (1.49 g, 21.89 mmol). After stirring at 65°C for 18 hours, the solvent was removed under reduced pressure and the resulting dark solid was dissolved in ethyl acetate (100 mL) and rinsed twice

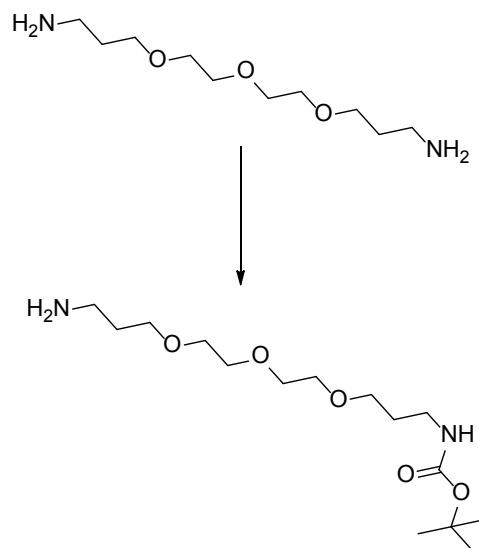
with equal volumes of water. The organic phase was separated, dried over magnesium sulfate and rotovaped to dryness. Purification by column chromatography (12% AcOH, 20% hexane, 68% EtOAc) gave 1.80 g of 6-(3-cyano-4-dicyanomethylene-1,2-dimethyl-cyclopent-2-enyl)-hexanoic acid as a yellow solid (Yield: 34%). IR (neat,  $\text{cm}^{-1}$ ): 2946, 2867, 2228, 1703, 1613, 1585, 1424, 1366, 1313, 1281, 1201, 1155, 1014, 934, 882;  $^1\text{H}$  NMR (400 MHz,  $\text{CDCl}_3$ )  $\delta$  2.39 (t, 2H, 6.8 Hz), 2.38 (s, 3H), 2.05 (m, 1H), 1.85 (m, 1H), 1.66 (m, 2H), 1.61 (s, 3H), 1.39 (m, 2H), 1.27 (m, 1H), 1.10 (m, 1H);  $^{13}\text{C}$  NMR (400 MHz,  $\text{CDCl}_3$ )  $\delta$  181.8, 178.7, 175.4, 110.9, 110.3, 108.8, 105.6, 102.0, 58.5, 37.1, 33.5, 28.5, 24.0, 23.4, 22.6, 14.2; HRMS  $m/z$  Calcd. for  $\text{C}_{16}\text{H}_{17}\text{N}_3\text{O}_3(\text{M}+\text{Na})$ : 322.1168. Found: 322.1141.

6-{4-Cyano-5-dicyanomethylene-2-methyl-3-[2-(4-nitro-phenyl)-vinyl]-2,5-dihydro-furan-2-yl}-hexanoic acid



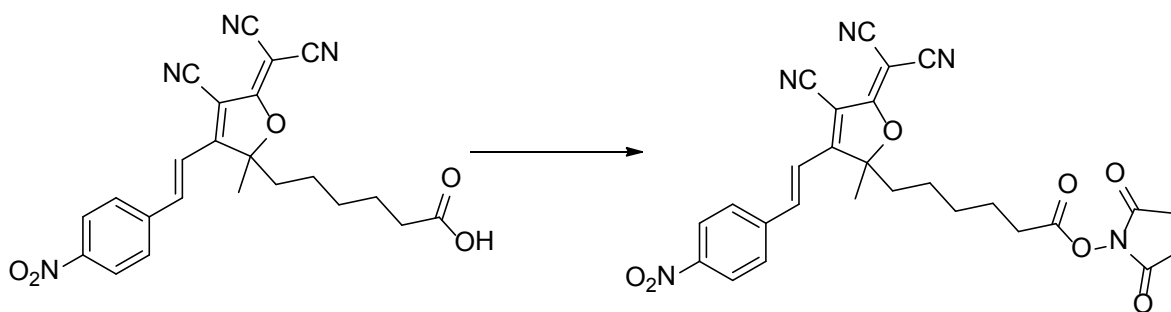
To a solution of 4-nitrobenzaldehyde (0.25 g, 1.65 mmol) in pyridine (15 mL) was added 6-(4-cyano-5-dicyanomethylene-2,3-dimethyl-2,5-dihydro-furan-2-yl)-hexanoic acid (0.30 g, 1.12 mmol) and 3 drops of acetic acid. After stirring at room temperature for 48 hours, the solution was treated dropwise with 2M HCl until copious amounts of green precipitates were formed. The precipitate was isolated by vacuum filtration and purified by column chromatography (58% EtOAc, 38% hexane, 4% AcOH) to give 0.22 g of 6-{4-cyano-5-dicyanomethylene-2-methyl-3-[2-(4-nitro-phenyl)-vinyl]-2,5-dihydro-furan-2-yl}-hexanoic acid as a yellow solid (Yield: 45%). IR (neat,  $\text{cm}^{-1}$ ): 3217, 3104, 3058, 2959, 2935, 2861, 2225, 1713, 1579, 1551, 1459, 1415, 1389, 1379, 1343, 1313, 1274, 1235, 1186, 1156, 1131, 1103, 1031, 1009, 982, 966, 939, 920, 881, 869, 845;  $^1\text{H}$  NMR (400 MHz, DMSO)  $\delta$  8.33 (d, 2H, 8.8 Hz), 8.18 (d, 2H, 8.8 Hz), 8.00 (d, 1H, 16.4 Hz), 7.42 (d, 1H, 16.4 Hz), 2.17 (t, 2H, 7.2 Hz), 1.80 (s, 3H), 1.46 (m, 2H), 1.24 (m, 5H), 1.09 (m, 1H);  $^{13}\text{C}$  NMR (400 MHz, DMSO)  $\delta$  177.3, 174.8, 173.9, 149.1, 144.0, 130.7, 124.6, 119.8, 112.8, 112.0, 110.8, 103.0, 102.5, 37.8, 33.8, 28.5, 24.5, 24.2, 22.7; HRMS  $m/z$  Calcd. for  $\text{C}_{30}\text{H}_{25}\text{N}_5\text{O}_8(\text{M}+\text{Na})$ : 455.1331. Found: 455.1331. Mp 171 C.

(3-{2-[2-(3-Amino-propoxy)-ethoxy]-ethoxy}-propyl)-carbamic acid tert-butyl ester



A solution of 4,7,10-trioxa-1,13-tridecanediamine (10.00 g, 45.39 mmol) in 60 mL of dichloromethane was brought to reflux. Over the course of 1 hour, (Boc)<sub>2</sub>O (1.98 g, 9.08 mmol) in 60 mL of dichloromethane was added dropwise. After refluxing for 24 hours the mixture was cooled to room temperature and rotovaped. Column chromatography (46% MeOH, 46% CH<sub>2</sub>Cl<sub>2</sub>, 8% NH<sub>4</sub>OH) of the resulting oil gave 2.47 g of the (3-{2-[2-(3-amino-propoxy)-ethoxy]-ethoxy}-propyl)-carbamic acid tert-butyl ester<sup>4</sup> as a yellow oil (Yield: 84%). IR (neat, cm<sup>-1</sup>): 3351, 2927, 2865, 1707, 1518, 1454, 1390, 1364, 1270, 1248, 1170, 1105, 1042, 980, 860, 778, 756; <sup>1</sup>H NMR (400 MHz, D<sub>2</sub>O) δ 3.60 (m, 8H), 3.50 (m, 4H), 3.06 (t, 2H, 6.8 Hz), 2.65 (t, 2H, 7.2 Hz), 2.15 (s, 1H), 1.66 (m, 4H), 1.35 (s, 9H).

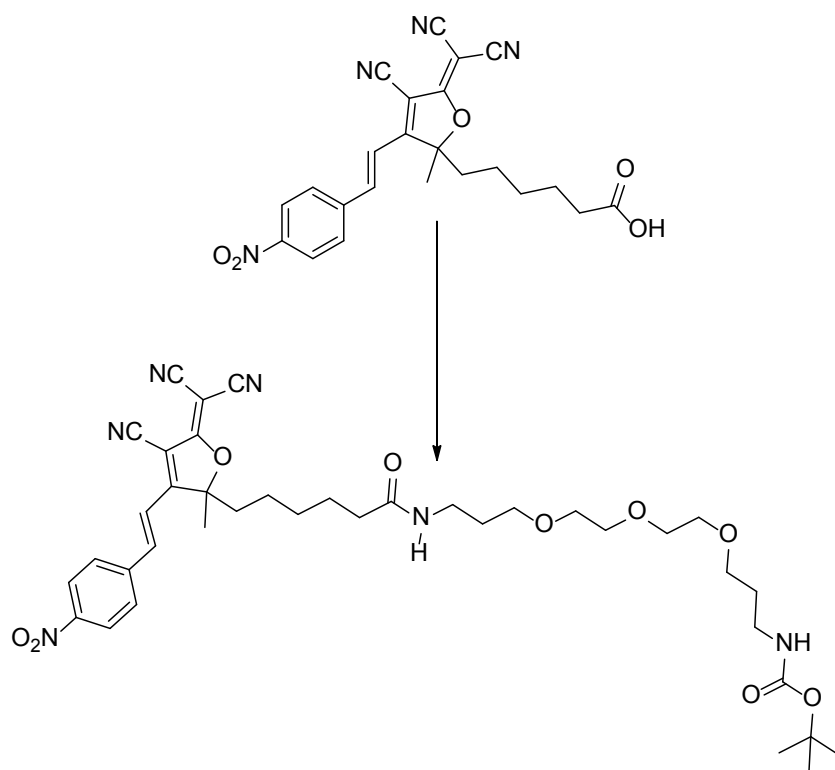
6-{4-Cyano-5-dicyanomethylene-2-methyl-3-[2-(4-nitro-phenyl)-vinyl]-2,5-dihydro-furan-2-yl}-hexanoic acid 2,5-dioxo-pyrrolidin-1-yl ester (4)



To a solution of 6-{4-cyano-5-dicyanomethylene-2-methyl-3-[2-(4-nitro-phenyl)-vinyl]-2,5-dihydro-furan-2-yl}-hexanoic acid (0.117 g, 0.270 mmol) in 30 mL of dichloromethane was added a solution of DCC (0.067 g, 0.325 mmol), DMAP (0.039 g, 0.325 mmol), and N-hydroxysuccinimide (0.037 g, 0.325 mmol). The resulting solution was allowed to stir at room temperature for 48 hours. Dicyclohexyl urea was removed by vacuum filtration and the resulting yellow solution was rotovaped to dryness and purified by column chromatography (EtOAc) giving 0.10 g of 6-{4-cyano-5-dicyanomethylene-2-methyl-3-[2-(4-nitro-phenyl)-vinyl]-2,5-

dihydro-furan-2-yl}-hexanoic acid 2,5-dioxo-pyrrolidin-1-yl ester as a yellow solid that contained substantial impurities in the aliphatic region when examined by  $^1\text{H}$ NMR. The solid was dissolved in 20 ml of dichloromethane and 15 ml of hexane. The mixture was rotovaped at room temperature and upon concentration the product precipitated. Vacuum filtration afforded 0.06 g of pure 6-{4-cyano-5-dicyanomethylene-2-methyl-3-[2-(4-nitro-phenyl)-vinyl]-2,5-dihydro-furan-2-yl}-hexanoic acid 2,5-dioxo-pyrrolidin-1-yl ester (Yield: 43%). IR (neat,  $\text{cm}^{-1}$ ): 2951, 2939, 2872, 2858, 2229, 1814, 1787, 1736, 1578, 1544, 1521, 1459, 1447, 1413, 1378, 1347, 1209, 1145, 1109, 1074, 1043, 972, 959, 883, 868, 841;  $^1\text{H}$  NMR (400 MHz, DMSO)  $\delta$  8.33 (d, 2H, 8.8 Hz), 8.18 (d, 2H, 8.8 Hz), 7.99 (d, 1H, 16.4 Hz), 7.42 (d, 1H, 16.4 Hz), 2.79 (s, 4H), 2.64 (t, 2H, 7.2 Hz), 2.21 (m, 2H), 1.81 (s, 3H), 1.61 (m, 2H), 1.35 (m, 2H), 1.27 (m, 1H), 1.18 (m, 1H);  $^{13}\text{C}$  NMR (400 MHz, DMSO)  $\delta$  177.3, 173.8, 170.6, 169.3, 149.1, 144.0, 140.9, 130.7, 124.5, 119.7, 112.8, 112.0, 110.8, 103.0, 102.4, 56.2, 37.8, 30.4, 28.1, 25.8, 24.3, 22.4; HRMS  $m/z$  Calcd. for  $\text{C}_{27}\text{H}_{23}\text{N}_5\text{O}_7$  (M+Na): 552.1495. Found: 552.1471.

[3-(2-{2-[3-(6-{4-Cyano-5-dicyanomethylene-2-methyl-3-[2-(4-nitro-phenyl)-vinyl]-2,5-dihydro-furan-2-yl}-hexanoylamino)-propoxy]-ethoxy}-ethoxy)-propyl]-carbamic acid tert-butyl ester (5)



To a solution of 6-{4-cyano-5-dicyanomethylene-2-methyl-3-[2-(4-nitro-phenyl)-vinyl]-2,5-dihydro-furan-2-yl}-hexanoic acid (0.075 g, 0.173 mmol) in dichloromethane (10 mL) was added DCC (0.043 g, 0.208 mmol), DMAP (0.025 g, 0.208 mmol) and (3-{2-[2-(3-amino-propoxy)-ethoxy]-ethoxy}-propyl)-carbamic acid tert-butyl ester (0.061 g, 0.191 mmol). After stirring for 48 hours at room temperature, the mixture was vacuum filtered and rotovapped to

dryness. The mixture was then subjected to column chromatography (90% EtOAc, 10% MeOH) to give 0.045 g of [3-(2-{2-[3-(6-{4-cyano-5-dicyanomethylene-2-methyl-3-[2-(4-nitro-phenyl)-vinyl]-2,5-dihydro-furan-2-yl]-hexanoylamino)-propoxy]-ethoxy}-ethoxy)-propyl]-carbamic acid tert-butyl ester as a sticky brown solid. Analysis by  $^1\text{H}$ NMR revealed that the material was pure (Yield: 35%). IR (neat,  $\text{cm}^{-1}$ ): 2935, 2865, 2227, 1738, 1649, 1579, 1520, 1452, 1366, 1343, 1228, 1216, 1089, 974, 867, 797;  $^1\text{H}$  NMR (400 MHz,  $\text{CDCl}_3$ )  $\delta$  8.33 (d, 2H, 8.8 Hz), 7.87 (d, 2H, 8.8 Hz), 7.77 (d, 1H, 16.8 Hz), 7.15 (d, 1H, 16.8 Hz), 6.35 (s, 1H), 4.96 (s, 1H), 3.60-3.50 (m, 12H), 3.33 (q, 2H, 6.0 Hz), 3.21 (q, 2H, 6.4 Hz), 2.23 (m, 1H), 2.13 (t, 2H, 7.2 Hz), 2.05 (m, 2H), 1.79 (s, 6H), 1.77 (m, 4H), 1.63 (m, 2H), 1.44 (s, 9H), 1.37 (m, 2H), 1.18 (m, 1H);  $^{13}\text{C}$  NMR (400 MHz,  $\text{CDCl}_3$ )  $\delta$  175.1, 172.6, 172.1, 156.0, 149.4, 143.5, 139.5, 129.6, 124.5, 118.6, 111.2, 110.5, 109.7, 102.9, 100.8, 70.4, 70.4, 70.1, 70.0, 69.4, 38.6, 38.4, 37.9, 36.0, 29.7, 28.9, 28.5, 28.4, 25.1, 24.6, 22.6; HRMS  $m/z$  Calcd. for  $\text{C}_{38}\text{H}_{50}\text{N}_6\text{O}_9$  (M+Na): 757.3539. Found: 757.3543.

### Bulk spectroscopy

Bulk solution absorption, emission, and excitation spectra were acquired on a Cary 6000i UV-vis NIR spectrophotometer and a Jobin-Yvon Horiba Fluorolog3 fluorimeter using standard 1-cm pathlength glass cuvettes. Molar absorption coefficients were quantified using dilutions of solutions with known concentrations. Fluorescence quantum yields ( $\Phi_F$ ) were referenced against standards with known quantum yields, and corrected for differences in optical density and solvent refractive index.<sup>5</sup> The optical density of samples for fluorescence quantum yield measurements was kept under 0.05 to avoid possible complications from aggregation, dimerization, or self-quenching. Fluorophores **2** and **3** in ethanol were measured against rhodamine 6G in ethanol ( $\Phi_F = 0.94$ ).<sup>6</sup>

Samples used to measure the bulk spectra in polymer films were prepared by doping a small amount of highly concentrated dye solution dissolved in toluene into a 10% (by mass) solution of poly(methyl methacrylate) (PMMA,  $T_g = 105^\circ\text{C}$ , MW = 75,000 g/mol, atactic, polydispersity  $\sim 2.8$ , PolySciences Inc.) and toluene. The solution was drop-cast onto a glass slide and allowed to solidify. The absorbance spectra were measured relative to an undoped film, with both slides placed orthogonal to the beam. Emission and excitation spectra were measured by orienting the slide to minimize scattered light and using the front-face detection geometry. Both absorption and emission spectra were measured at several film locations, and with several different film preparations, to compensate for unevenness in polymer thickness.

The steady-state enzyme kinetics of NTR with nitro compounds **1** and **5** were monitored spectrophotometrically by following the initial rate of **2** formation at 500 nm ( $\Delta\epsilon_{500} = 15200 \text{ M}^{-1} \text{ cm}^{-1}$ ) in PBS (pH 7.4). Because of its enhanced water solubility, **5** was used instead of **1** for quantitative kinetic measurements. It was assumed that the extinction coefficient for the product fluorophore from the reaction of **5** with NTR was the same as the extinction coefficient of **2** from the spectral similarity of the NTR product mixture.  $\beta$ -Nicotinamide adenine dinucleotide (NADH, 97% pure, Sigma Aldrich) and **5** were mixed in a 3 mL glass cuvette, and then the reaction was initiated by adding a small amount of nitroreductase enzyme (NTR, >90% pure,



Sigma Aldrich) (final concentration ~10 nM). The substrate concentrations ranged from 0-130  $\mu\text{M}$  of NADH and 0-8  $\mu\text{M}$  of **5**; these concentrations were determined by molar absorptivity ( $\epsilon_{420} = 6220 \text{ M}^{-1} \text{ cm}^{-1}$  for NADH,<sup>7</sup>  $\epsilon_{390} = 22600 \text{ M}^{-1} \text{ cm}^{-1}$  for **5**) or by mass measurements. All initial rates were measured in triplicate and the standard deviation of the measured rates was used to calculate the standard error of the mean for the fitted kinetic parameters. Analysis of the kinetic data was performed using nonlinear regression with equal weighting of all points to the ping-pong bi-bi equation (eq 1 in paper) using a bespoke Matlab program.

### ***In vitro* sample preparation and analysis**

The polymer samples used to measure bulk photostability and to quantify the average emitted photons per single molecule were prepared using 1% (by mass) solutions of poly(vinyl alcohol-vinyl acetate) (PVA, 88% hydrolyzed, MW ~31,000 g/mol, Polysciences Inc.) in Nanopure water. The polymer sample was doped with nanomolar concentrations of fluorophores, and then spin-cast onto Argon-plasma-etched glass coverslips. Plasma-etching with argon was necessary to remove fluorescent impurities.

Poly-L-lysine coated coverslips were made following the instructions from the manufacturer (Sigma Aldrich). Ar-plasma-etched glass slides were incubated in a 1:10 dilution of poly-L-lysine (0.1% w/v in water, Sigma Aldrich) with Nanopure water for 5 minutes, and then dried at 60°C for 1 hour. The poly-lysine coated coverslips were then labeled with the NHS-fluorogen **4** by incubating with **4** (32  $\mu\text{M}$ ) in sodium carbonate buffer (0.1M, pH 8.55) for 5 minutes. The slides were then washed 3x with sodium carbonate buffer followed by 3 washings with PBS buffer (pH 7.5). The final sample was immersed in PBS buffer using a silicon isolator chamber and then imaged with an irradiance of 0.64 kW/cm<sup>2</sup>. NADH and NTR enzyme were added to the isolator chamber to obtain final concentrations of 10  $\mu\text{M}$  and 1  $\mu\text{M}$ , respectively.

The photobleaching quantum yield ( $\Phi_B$ ) was determined using PVA polymer samples doped with ~100 nM dye and the procedure outlined in reference<sup>1</sup>.

$\Phi_B$  is the probability of photobleaching after absorbing a photon, or the ratio of the bleaching rate  $R_B$  to the rate of absorbing photons  $R_{\text{abs}}$ :

$$\Phi_B = \frac{R_B}{R_{\text{abs}}} = \frac{1}{\tau_B R_{\text{abs}}} = \frac{1}{\tau_B I_\lambda \sigma_\lambda \left( \frac{\lambda}{hc} \right)} \quad (\text{S1})$$

where  $\tau_B$  is the decay constant of the single exponential fit to the bulk fluorescence decay of dye-doped polymers,  $\sigma_\lambda$  is the absorption cross-section (related to the molar absorption coefficient by  $\sigma_\lambda = (1000)2.303\epsilon_\lambda / N_A$ ),  $I_\lambda$  is the irradiance at the sample,  $\lambda$  is the excitation wavelength,  $h$  is Planck's constant and  $c$  is the speed of light. Smaller values of  $\Phi_B$  indicate greater photostability.

The total number of detected photons per molecule ( $N_{\text{tot}}$ ) was extracted from single-molecule time traces of fluorescence emission by spatially and temporally integrating all of the photons (minus background) contributing to the single-molecule spot. The results from hundreds of single molecules were plotted versus a probability distribution ( $P_N = m_N/M$ ) and the average number of detected photons was extracted from a single exponential fit. The probability distribution  $P_N$  is the ratio of the number of SMs  $m_N$  surviving after a given number of emission cycles  $N$  to the total number of molecules  $M$  in the measurement set.<sup>1, 8</sup> This approach gives comparable results to histogramming the detected photons,<sup>9</sup> but avoids binning artifacts. To convert photons detected to total emitted photons, the measured value for detected photons is divided by the optical system collection efficiency<sup>10</sup> of 0.04.

### Microscopy

Samples were imaged using an Olympus IX71 inverted microscope in an epifluorescence configuration<sup>10</sup> using 532 nm illumination from a diode-pumped laser (CrystaLaser, max output 500 mW). Sample irradiances ranged from 0.64 kW/cm<sup>2</sup> to 15 kW/cm<sup>2</sup> (determined by measuring power at stage with Newport power meter (model 1918-C) and estimating the FWHM spot size by fitting an average uniform fluorescence image to a 2D Gaussian by nonlinear least squares in a bespoke Matlab program). The sample emission was collected through a 100x, 1.4 N.A. oil-immersion objective, scattered excitation light was removed by filtering through either a 540DRLP or a 532DCLP dichroic followed by BrightLine 593/40 and 700AGSP emission filters (Semrock) and finally imaged onto a 512x512 pixel electron-multiplication Si EMCCD camera (Andor iXon+) with integration times ranging from 8 ms to 100 ms. The ADC counts recorded by the EMCCD camera were converted to detected photons using the conversion gain (number of electrons after on-chip gain)/(ADC count) and the electron multiplication gain (number of electrons after on-chip gain)/(number of photoelectrons). The conversion gain of the camera (24.9 electrons/count) and the electron multiplication gain (ranged from 25-300) were measured following previously described procedures.<sup>11, 12</sup>

### Live-cell imaging and analysis

Cells used in live-cell imaging were first grown overnight in 5 mL of PYE growth medium,<sup>13</sup> then diluted (5  $\mu$ L / 5 mL) into clean M2G minimal fluorescence buffer.<sup>14</sup> This dilution into fresh M2G was repeated after the cell suspension reached an OD  $\sim$  0.3 until cells had grown for at least 48 hours in clean M2G. This step reduced cellular autofluorescence. Amounts of **1** in DMSO ranging in concentration from  $\sim$ nM (for SM samples) to  $\sim$  $\mu$ M (for bulk samples) were added to the cells and allowed to incubate for times ranging from 1 minute to 20 minutes. When menadione was necessary for the specific sample, it was added simultaneously with **1**. After the incubation period, cells were washed 2x by centrifuging for 3 minutes at 8,000 RPM, and then removing the supernatant and replacing it with clean M2G.

The agarose pads used for imaging were made by heating 1.5% (by mass) low melting-point agarose (Invitrogen) in M2G buffer, then sandwiching 400  $\mu\text{L}$  agarose solution between two Argon-plasma-etched glass coverslips (35x35 mm). After the agarose had cooled and solidified, one glass coverslip was removed and 1  $\mu\text{L}$  of washed cells were pipetted on the agarose. The agarose pad with cells was flipped onto a large Argon-plasma-etched clean glass slide and the edges between the two coverslips were sealed with wax. The cells were imaged through the large glass slide.

Cell samples for bulk fluorescence imaging were prepared by a 30 minute incubation with **1** (5  $\mu\text{L}$ ), **1** and menadione (0.2 mM), or menadione alone and compared to a sample without any additives. Each condition was done in triplicate and incubation times were kept within 5 minutes of each other. The cells were grown and washed as described above, and placed on agarose pads. Imaging was performed as described above with a laser power of 2.5  $\text{kW}/\text{cm}^2$  at the sample and an integration time of 100 ms.

Cell samples for SM and SR imaging were prepared by a 2 minute incubation with nM amounts of **1**, then washed and placed on an agarose pad as described above. Samples were imaged as outlined previously, with a laser power of 15  $\text{kW}/\text{cm}^2$  at the sample and integration times ranging from 8 ms to 100 ms. The fluorescence from cell samples without **1** was measured for each experiment to check for possible fluorescent contamination.

The average photons detected per cell (Figure 4E) was determined using a bespoke script in the image processing software program ImageJ which converted average white light images of cells to binary masks. The binary mask was multiplied with the fluorescence image to remove any background fluorescence and retain only fluorescence arising from cells. The average integrated fluorescence from the cells was divided by the total number of cells to obtain an average value for individual cell fluorescence.

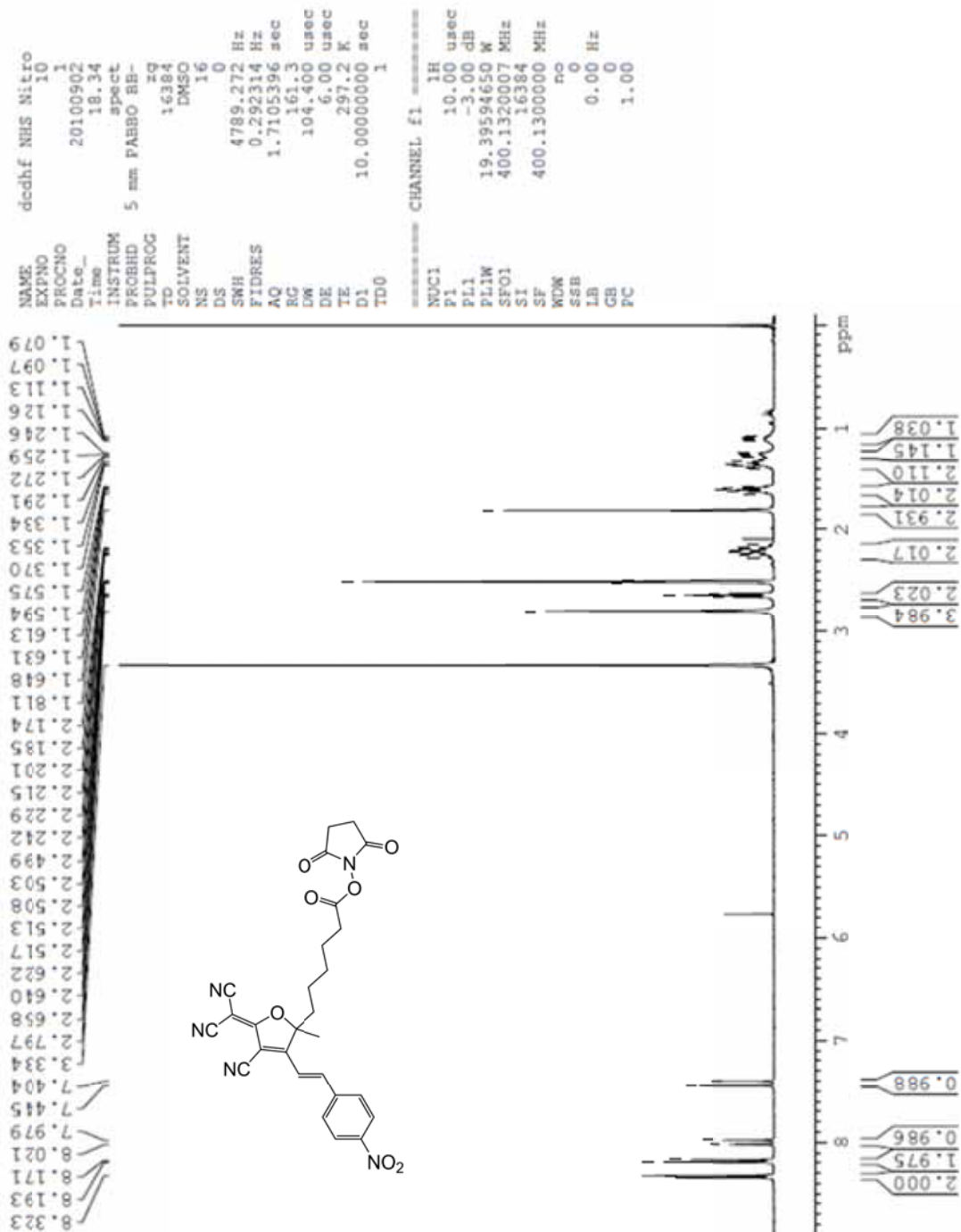
Superresolution image reconstructions were obtained from image stacks with the average cell background subtracted using previously published image processing techniques.<sup>15-17</sup> The position of each single emitter was determined by fitting the signal above background (in a small region of interest containing the emitter) to a 2D Gaussian with nonlinear least squares regression analysis (nlinfit, in MATLAB). The fitting function determined background, amplitude, width, x-center and y-center. The SM fits were checked by hand by comparing the raw data to the fitted positions. The remaining good fits were re-plotted to form the reconstruction using a macro written in ImageJ as 2D Gaussian profiles using the average statistical error of the localizations (96% confidence interval, averaged over all single-molecule localizations) of  $17.9 \pm 0.3$  nm and weighting each localization with its measured integrated intensity.

## References

- 1 S. J. Lord, N. R. Conley, H. - D. Lee, R. Samuel, N. Liu, R. J. Twieg and W. E. Moerner, *J. Am. Chem. Soc.*, 2008, **130**, 9204-9205 (DOI:10.1021/ja802883k).
- 2 M. Davis, A. Chafin, R. Hollins, L. Baldwin, E. Erickson, P. Zarras and E. Drury, *Synth. Commun.*, 2004, **34**, 3419-3429.
- 3 R. Mujumdar and R. West, *Chiral indole intermediates and their fluorescent cyanine dyes containing functional groups*, 2004.
- 4 F. Menger, J. Bian and V. Seredyuk, *Angew. Chem. Int. Ed.*, 2004, **43**, 1265-1267.
- 5 J. R. Lakowicz, *Principles of fluorescence spectroscopy*, Springer Science, New York, 2006.
- 6 M. Fischer and J. Georges, *Chem. Phys. Lett.*, 1996, **260**, 115-118.
- 7 Y. Galante and Y. Hatefi, *Methods Enzymol.*, 1978, **53**, 15-21.
- 8 A. Molski, *J. Chem. Phys.*, 2001, **114**, 1142-1147 (DOI:10.1063/1.1333760).
- 9 B. L. Lounis, J. Deich, F. I. Rosell, S. G. Boxer and W. E. Moerner, *J. Phys. Chem. B*, 2001, **105**, 5048-5054.
- 10 W. E. Moerner and D. P. Fromm, *Rev. Sci. Instrum.*, 2003, **74**, 3597-3619.
- 11 M. Newberry, *Mirametrics Technical Note on Pixel Response Effects in CCD Camera Gain Calibration* [http://www.mirametrics.com/tech\\_note\\_ccdgain.htm](http://www.mirametrics.com/tech_note_ccdgain.htm), 1998.
- 12 M. A. Thompson, M. D. Lew, M. Badieirostami and W. E. Moerner, *Nano Lett.*, 2010, **10**, 211-218 (DOI:10.1021/nl903295p).
- 13 J. S. Poindexter, *Microbiol. Mol. Biol. Rev.*, 1964, **28**, 231-295.
- 14 B. Ely, *Meth. Enzymol.*, 1991, **204**, 372-384.
- 15 M. A. Thompson, J. S. Biteen, S. J. Lord, N. R. Conley and W. E. Moerner, *Meth. Enzymol.*, 2010, **475**, 27-59.
- 16 J. S. Biteen, M. A. Thompson, N. K. Tselentis, G. R. Bowman, L. Shapiro and W. E. Moerner, *Nat. Methods*, 2008, **5**, 947-949.
- 17 J. S. Biteen, M. A. Thompson, N. K. Tselentis, L. Shapiro and W. E. Moerner, *Proc. SPIE*, 2009, **7185**, 71850I.

### Proton NMR spectra

6-{4-Cyano-5-dicyanomethylene-2-methyl-3-[2-(4-nitro-phenyl)-vinyl]-2,5-dihydro-furan-2-yl}-hexanoic acid 2,5-dioxo-pyrrolidin-1-yl ester





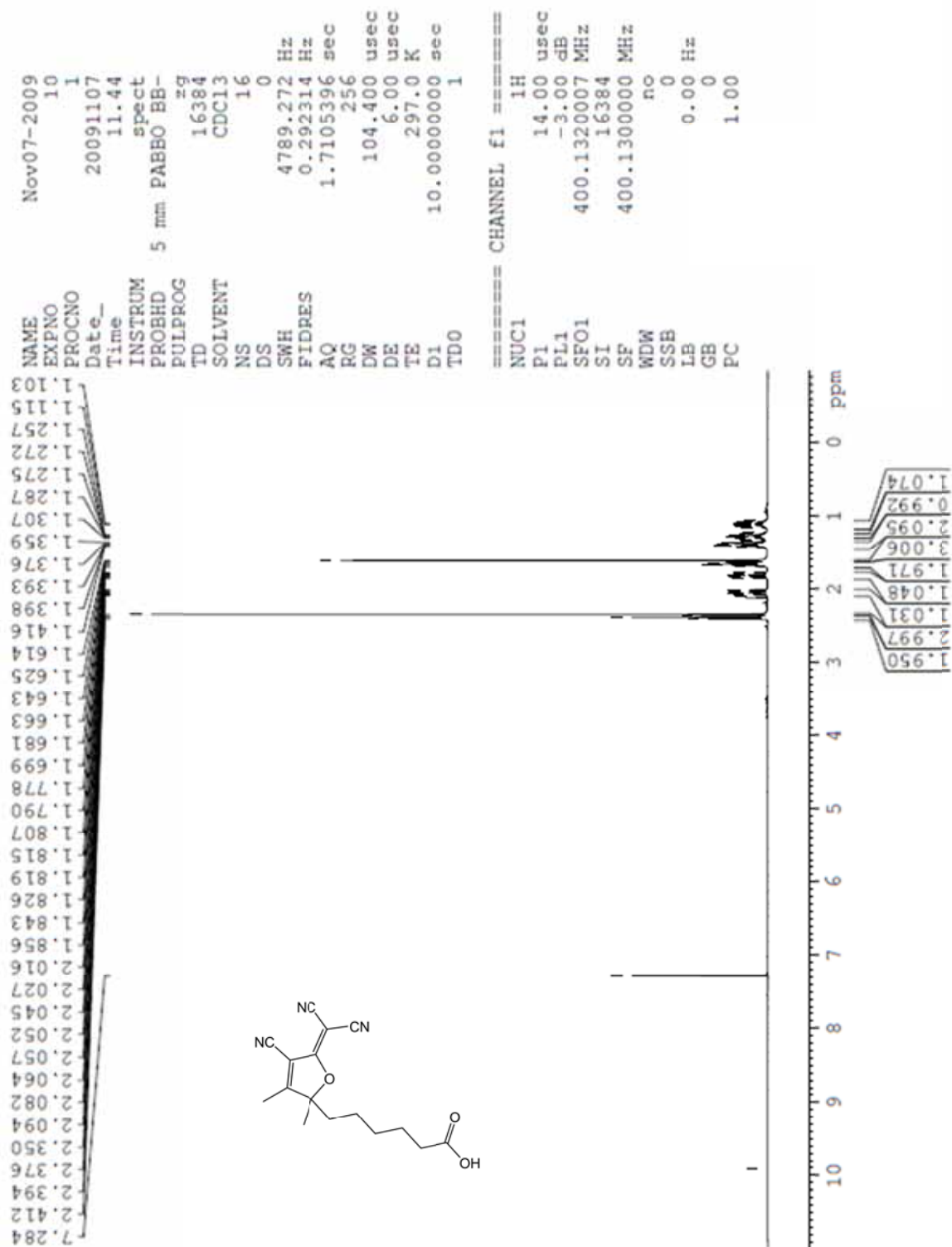


6-{4-Cyano-5-dicyanomethylene-2-methyl-3-[2-(4-nitro-phenyl)-vinyl]-2,5-dihydro-furan-2-yl}-hexanoic acid

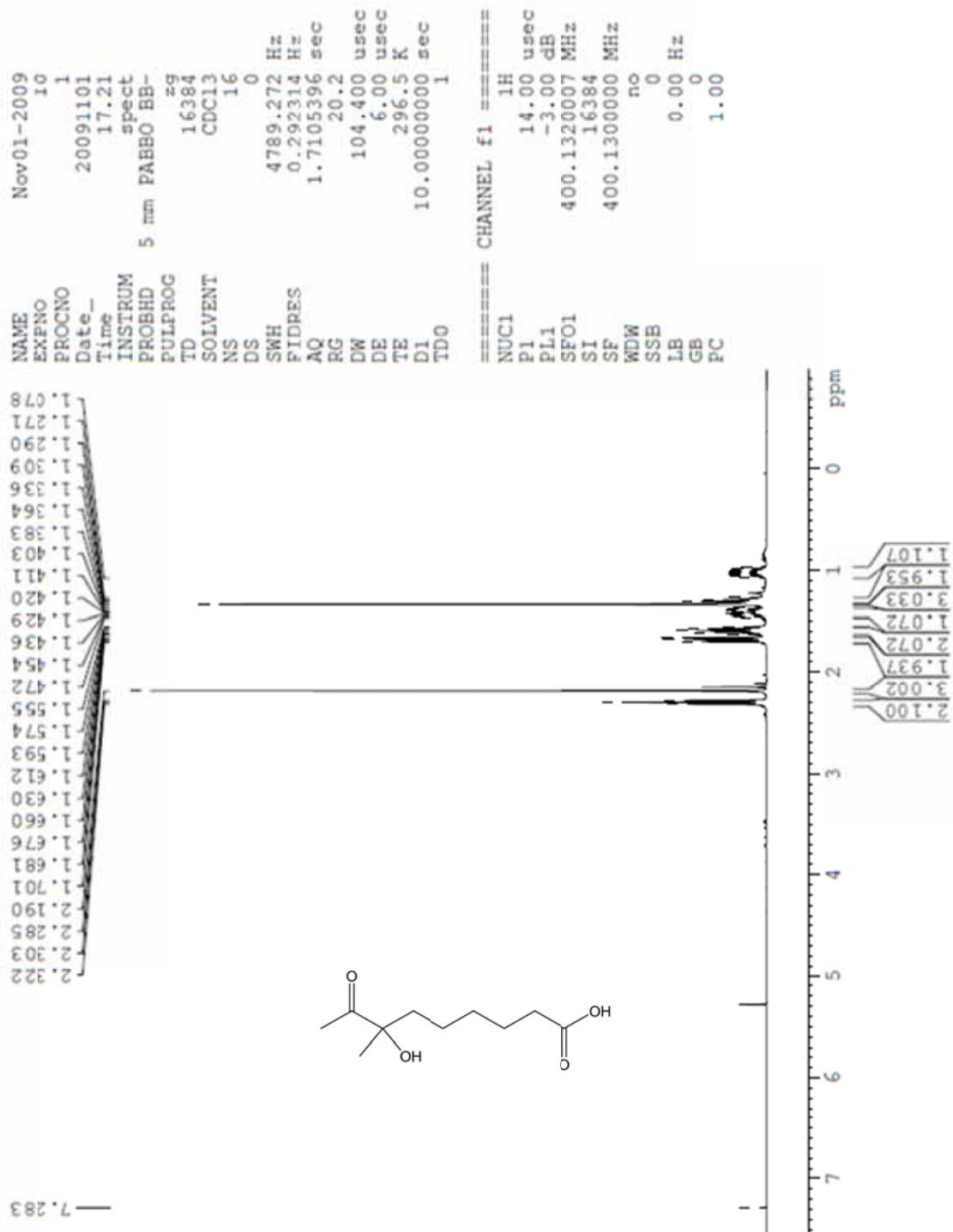




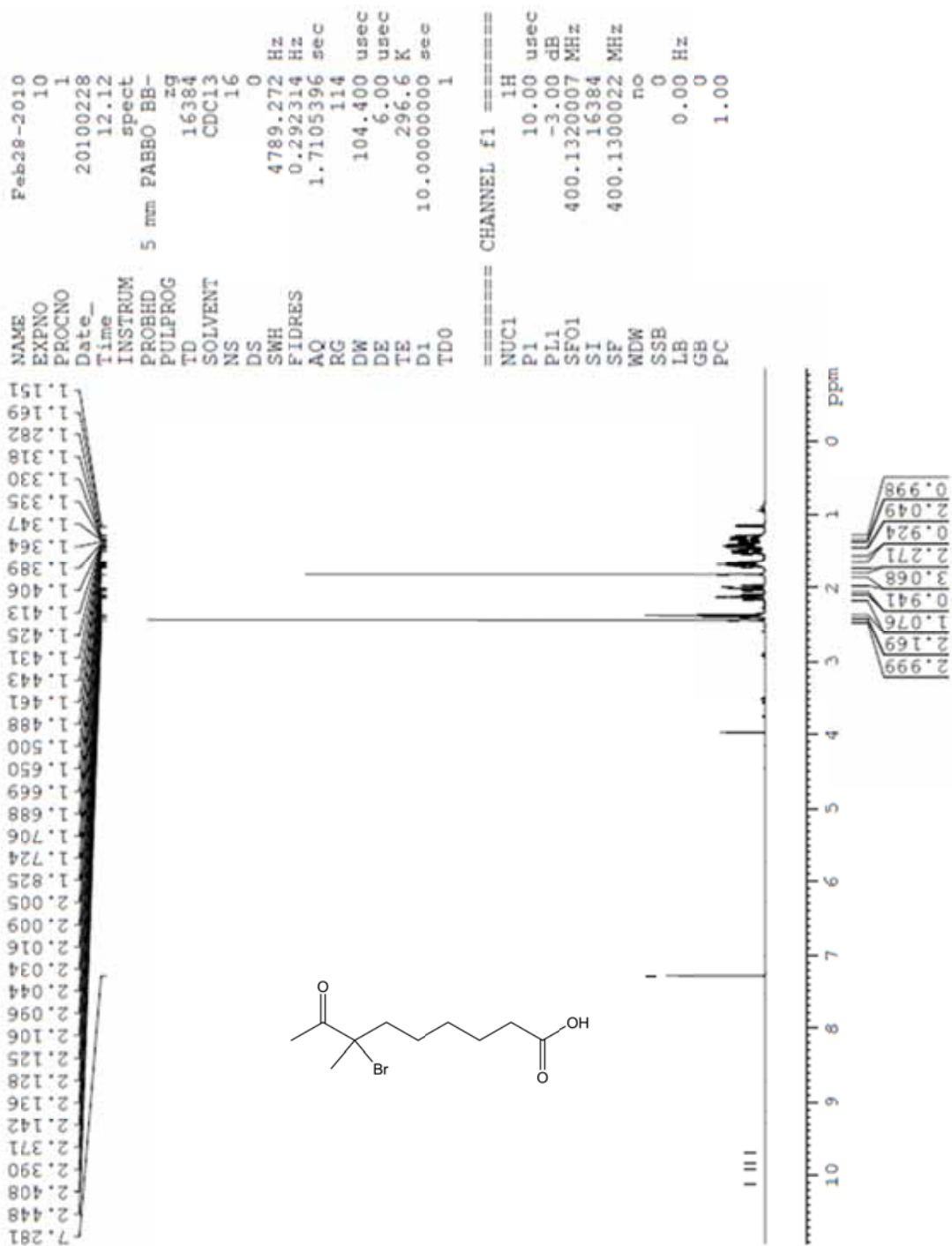
6-(3-Cyano-4-dicyanomethylene-1,2-dimethyl-cyclopent-2-enyl)-hexanoic acid



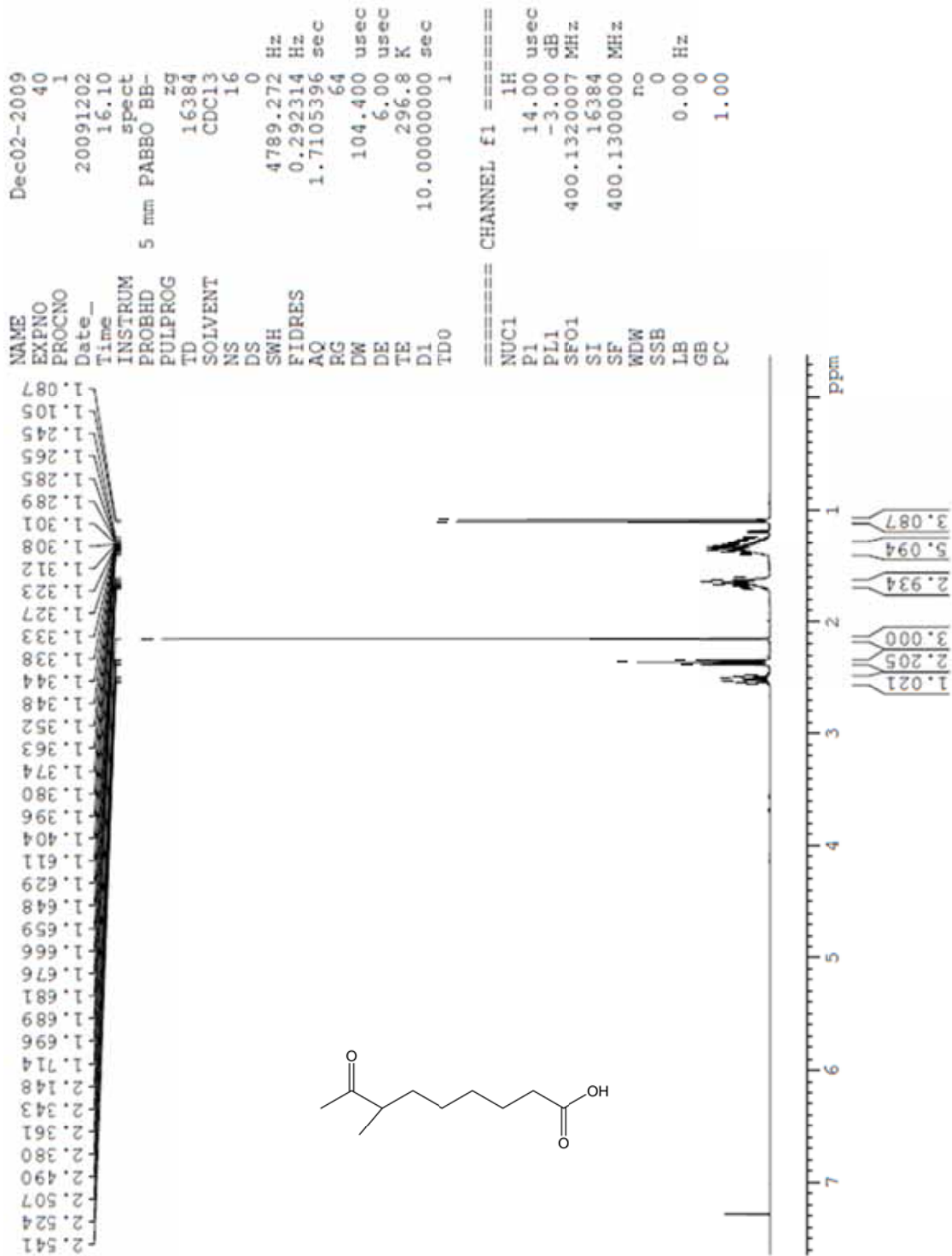
### 7-hydroxy-7-methyl-8-oxo-nonanoic acid



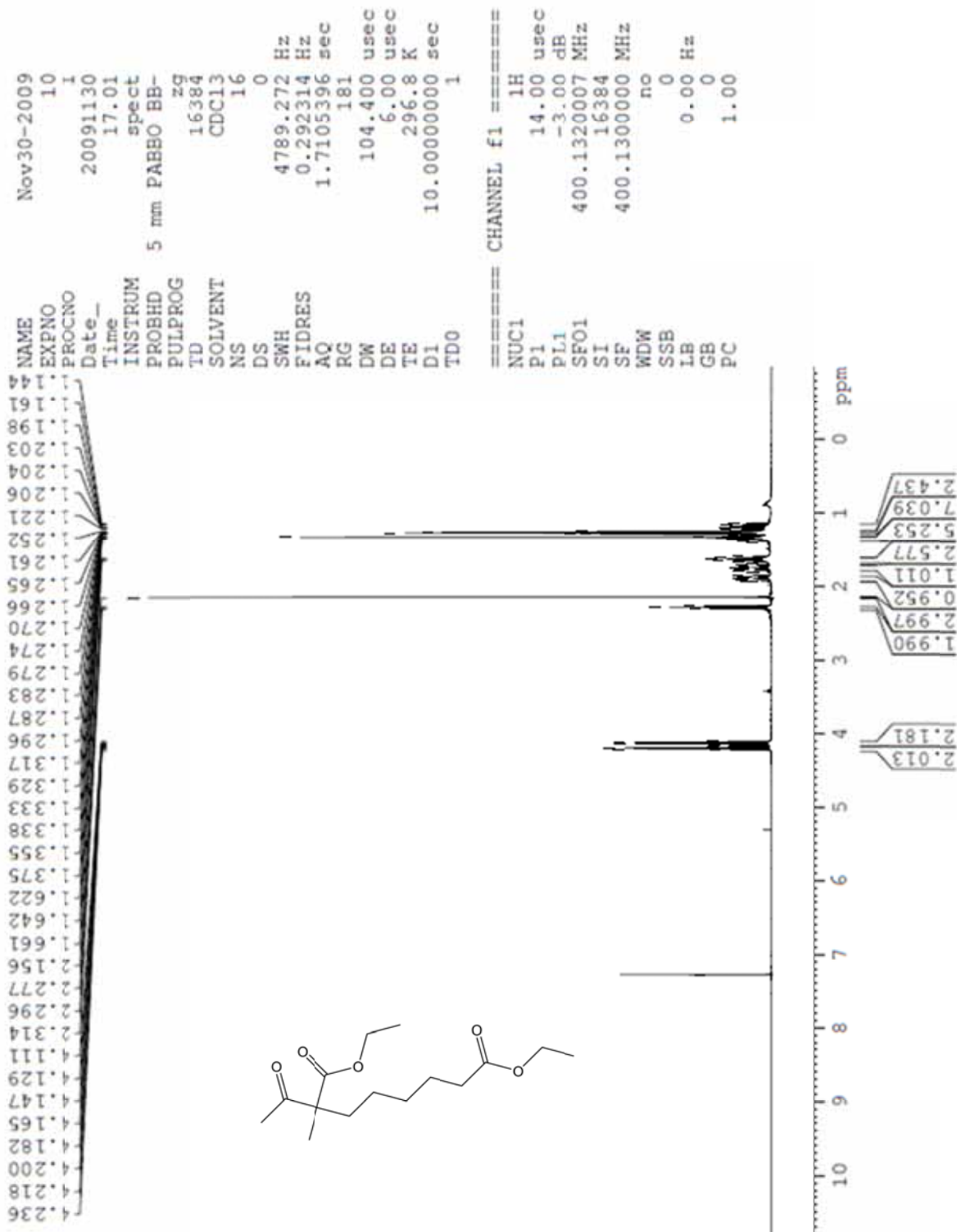
### 7-Bromo-7-methyl-8-oxo-nonanoic acid



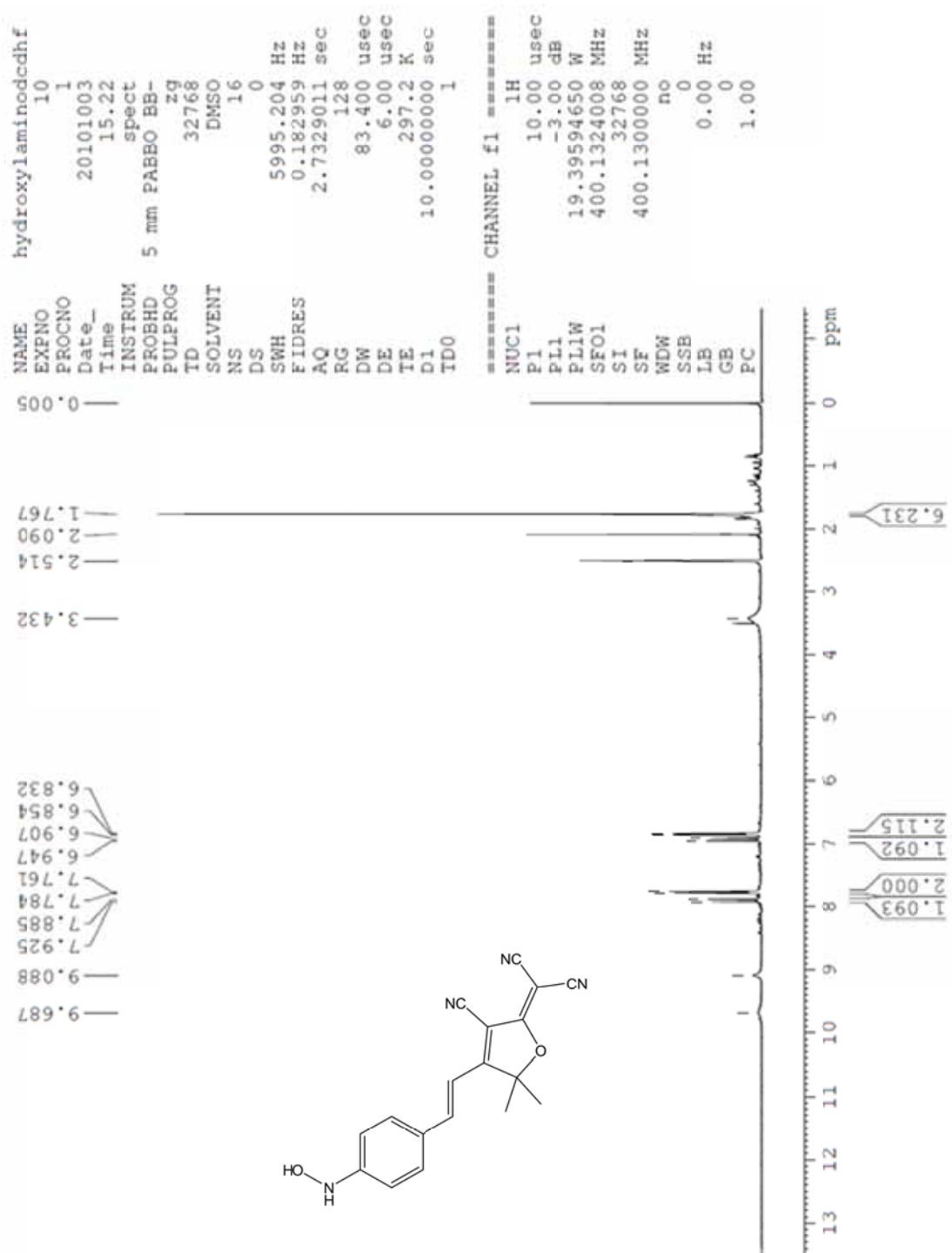
### 7-Methyl-8-oxo-nonanoic acid



### 2-Acetyl-2-methyl-octanedioic acid diethyl ester



2-{3-Cyano-4-[2-(4-hydroxyamino-phenyl)-vinyl]-5,5-dimethyl-5H-furan-2-ylidene}-malononitrile



2-{3-Cyano-5,5-dimethyl-4-[2-(4-nitro-phenyl)-vinyl]-5H-furan-2-ylidene}-malononitrile<sup>2</sup>

